The International Journal of Cardiovascular Imaging (2023) 39:1927–1941
https://doi.org/10.1007/s10554-023-02905-y

ORIGINAL PAPER

Calcified plaque harboring lipidic materials associates with no-reflow phenomenon after PCI in stable CAD

Hayato Hosoda[1] · Yu Kataoka[2] · Stephen J. Nicholls[3] · Rishi Puri[4] · Kota Murai[2] · Satoshi Kitahara[2] · Kentaro Mitsui[2] · Hiroki Sugane[1] · Kenichiro Sawada[2] · Takamasa Iwai[2] · Hideo Matama[2] · Satoshi Honda[2] · Kensuke Takagi[2] · Masashi Fujino[2] · Shuichi Yoneda[2] · Fumiyuki Otsuka[2] · Itaru Takamisawa[5] · Kensaku Nishihira[6] · Yasuhide Asaumi[2] · Kazuya Kawai[1] · Teruo Noguchi[2]

Received: 15 December 2022 / Accepted: 19 June 2023 / Published online: 28 June 2023

Abstract

Calcified atheroma has been viewed conventionally as stable lesion which less likely increases no-reflow phenomenon. Given that lipidic materials triggers the formation of calcification, lipidic materials could exist within calcified lesion, which may cause no-reflow phenomenon after PCI. The REASSURE-NIRS registry (NCT04864171) employed near-infrared spectroscopy and intravascular ultrasound imaging to evaluate maximum 4-mm lipid-core burden index ($maxLCBI_{4mm}$) at target lesions containing small (maximum calcification arc < 180°: n = 272) and large calcification (maximum calcification arc ≥ 180°: n = 189) in stable CAD patients. The associations of $maxLCBI_{4mm}$ with corrected TIMI frame count (CTFC) and no-reflow phenomenon after PCI were analyzed in patients with target lesions containing small and large calcification, respectively. No-reflow phenomenon occurred in 8.0% of study population. Receiver-operating characteristics curve analyses revealed that optimal cut-off values of $maxLCBI_{4mm}$ for predicting no-reflow phenomenon were 585 at small calcification (AUC = 0.72, p < 0.001) and 679 at large calcification (AUC = 0.76, p = 0.001). Target lesions containing small calcification with $maxLCBI_{4mm} \geq 585$ more likely exhibited a greater CTFC (p < 0.001). In those with large calcification, 55.6% of them had $maxLCBI_{4mm} \geq 400$ [vs. 56.2% (small calcification), p = 0.82]. Furthermore, a higher CTFC (p < 0.001) was observed in association with $maxLCBI_{4mm} \geq 679$ at large calcification. On multivariable analysis, $maxLCBI_{4mm}$ at large calcification still independently predicted no-reflow phenomenon (OR = 1.60, 95%CI = 1.32–1.94, p < 0.001). $MaxLCBI_{4mm}$ at target lesions exhibiting large calcification elevated a risk of no-reflow phenomenon after PCI. Calcified plaque containing lipidic materials is not necessarily stable lesion, but could be active and high-risk one causing no-reflow phenomenon.

Keywords Calcification · Lipid plaque component · No-reflow · Stable coronary artery disease · Percutaneous coronary intervention

✉ Yu Kataoka
yu.kataoka@ncvc.go.jp

[1] Department of Cardiovascular Medicine, Chikamori Hospital, Kochi, India

[2] Department of Cardiovascular Medicine, National Cerebral and Cardiovascular Center, 6-1, Kishibe-Shimmachi, Suita, Osaka 564-8565, Japan

[3] MonashHeart, Monash University, Melbourne, Australia

[4] Department of Cardiovascular Medicine, Cleveland Clinic, Cleveland, OH, USA

[5] Department of Cardiovascular Medicine, Sakakibara Heart Institute, Fuchyu, Tokyo, Japan

[6] Department of Cardiology, Miyazaki Medical Association Hospital, Miyazaki, Japan

Abbreviations

CAD	Coronary artery disease
CI	Confidence interval
CTFC	Corrected thrombolysis in myocardium infarction frame count
DES	Drug-eluting stent
IVUS	Intravascular ultrasound
$MaxLCBI_{4mm}$	Maximum 4-mm lipid-core burden index
NIRS	Near-infrared spectroscopy
OR	Odds ratio
PCI	Percutaneous coronary intervention

Introduction

Lipidic plaque component is an important feature of coronary atheroma which elevates a risk of no-reflow phenomenon after PCI with stent implantation [1–3]. By contrast, calcified atheroma has been viewed conventionally as stable lesion which less likely causes this PCI-related complication. However, pathophysiologically, the formation of calcification is triggered by lipidic plaque components which induce osteogenic differentiation and inflammatory cytokines [4–9]. These features suggest that lipidic plaque materials could exist within calcified lesions, which may associate with deterioration of coronary flow after PCI. A combination catheter of intravascular ultrasound (IVUS) and near-infrared spectroscopy imaging (NIRS) is an intravascular imaging modality which enables to quantitatively visualize lipidic burden within calcified atheroma in vivo [10–14]. Therefore, the current study investigated no-reflow phenomenon after stent implantation at calcified atheroma containing lipidic plaque materials in stable CAD patients by using NIRS/IVUS imaging.

Methods

REASSURE-NIRS registry

The REASSURE-NIRS registry is a multi-center prospective registry which consecutively enrolled patients with CAD who received PCI with NIRS/IVUS imaging (NCT04864171). A total of 529 patients with stable CAD have been enrolled in this registry from 1st of August, 2015 to 31st of December, 2021. Of these, the following subjects were excluded; subjects with in-stent restenosis at target lesions (n = 15), those with target lesion at bypass graft (n = 4), those who had lesions with non-superficial calcification only (n = 20), those who did not receive pre NIRS/IVUS imaging due to the need for pre-dilatation or debulking procedures first (n = 18), those who did not receive stent implantation (n = 29) and those with insufficient image quality (n = 2). As a consequence, the remaining 461 stable CAD patients with de novo target lesions who received PCI with drug-eluting stent (DES) implantation and NIRS/IVUS imaging were included into the current analysis (Fig. 1). Target lesion was angiographically identified. Of these, target lesions exhibiting moderate stenosis were evaluated by FFR for indication of PCI. Fractional flow reserve < 0.80 was defined as the presence of myocardial ischemia requiring PCI. Stable CAD included angina pectoris and silent myocardial ischemia. Silent myocardial ischemia was defined as fractional flow reserve ≤ 0.80. This study was approved by the institutional review board of the National Cerebral and Cardiovascular Center (M30-084-4), the Miyazaki Medical Association Hospital (2020-43) and Sakakibara Heart Institute.

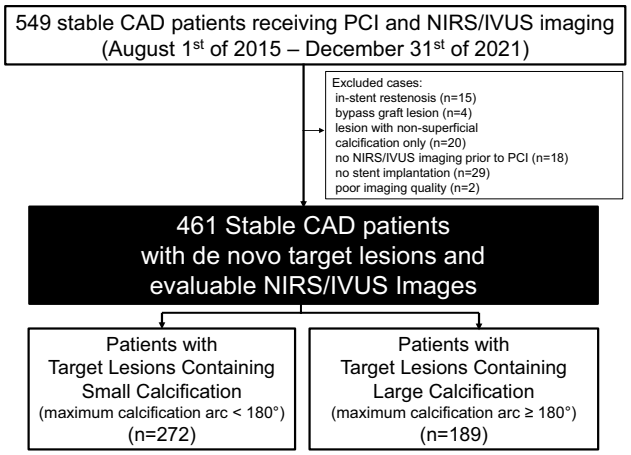

Fig. 1 Patients' disposition. The current study included stable CAD patients with de novo target lesions and evaluable NIRS/IVUS images. Patients were stratified into two groups according to maximum calcification arc < (small calcification) and ≥ 180° (large calcification). *CAD* coronary artery disease, *IVUS* intravascular ultrasound, *NIRS* near-infrared spectroscopy, *PCI* percutaneous coronary intervention

Coronary angiographic analysis and definition of no-reflow phenomenon

Coronary angiography was performed with a frame rate of 30/s. Corrected Thrombolysis In Myocardium Infarction frame count (CTFC) was measured immediately after stent implantation [15, 16]. In patients with thrombolysis in myocardium infarction flow grade 0 or 1 after PCI, a CTFC of 100 was used. No-reflow phenomenon was defined as CTFC > 27 on coronary angiography without mechanical obstruction of coronary artery after stent implantation [15, 16]. In patients who received filter-wire (Parachute™, GoodCare, Nagoya, Japan) prior to stent implantation, the occurrence of filter no-reflow was considered as no-reflow phenomenon. Coronary angiography was evaluated by two independent physicians (YK and KK). Quantitative coronary angiography (QCA) analysis was performed at target lesions by using off-line commercially available software (QAngio® XA, Medis, Leiden, the Netherlands). QCA analysis included reference vessel diameter, minimal lumen diameter, percent diameter stenosis and lesion length.

PCI procedures and NISR/IVUS imaging

In the current study, target lesion was defined as the lesion where PCI was performed. All procedural decisions including the selection of DES, filter-wire and other devices, the use of mechanical support system and adjunctive pharmacotherapy were made according to the discretion of the individual PCI operator. Each PCI operator was encouraged to optimize stent expansion at target lesion, which was defined as (1) minimum stent area (MSA) > 5.0 mm^2 or larger than distal reference lumen area on IVUS imaging, (2) IVUS-derived plaque area at the proximal and distal edge of the stents < 50%, and (3) no edge dissection which involves media with a length > 3 mm on IVUS imaging [17].

NIRS/IVUS imaging was conducted prior to PCI to analyze lipidic and calcific features at target lesions. In detail, after intracoronary administration of nitroglycerin (100-300ug), the imaging catheter (TVC Insight™ or Dualpro™, Infraredx, Bedford, MA, USA) was advanced into the target vessel and the catheter positioned distal to an angiographically identifiable target lesions. NIRS/IVUS imaging catheter was automatically withdrawn at a translation velocity of 0.5 mm/sec and 960 rpm (TVC Insight™) or 2.0 mm/sec and 1800 rpm (Dualpro™).

Quantitative analysis of calcification and lipidic plaque components at target lesions on NIRS/IVUS imaging

The raw IVUS data was transferred to commercially available software, QIvus® (Medis, Leiden, the Netherlands) for quantitative analysis of IVUS images. Makoto® system (Infraredx, Bedford, MA, USA) was used to analyze obtained chemogram data on NIRS imaging. Both analyses were conducted by persons who were blinded to the clinical characteristics of the patients (HH, TI, KM, SK, KK and YK). Quantitative measurements were conducted to evaluate the degree of lipidic and calcific plaque materials at target lesions.

Calcification

Calcification was identified by an echogenic signal brighter than the adventitia with corresponding acoustic shadowing [18]. The arc of calcification was measured at every-1 mm cross-sectional image at target lesions. Small and large calcifications were defined as maximum calcification arc at target lesions < and ≥ 180°, respectively.

Lipidic plaque component

Lipidic plaque component was measured by using NIRS images. Throughout obtained raw spectra, a probability of lipid core on NIRS imaging was automatically mapped to a red-to-yellow color scale. Then, maximum 4-mm lipid-core burden index ($maxLCBI_{4mm}$) was calculated as the number of yellow pixels within target lesions, divided by the total pixel quantity within the corresponding segments [10–13].

Statical analysis

Continuous values with normal distribution were expressed as mean ± SD. Normality of distribution was tested with the Shapiro–Wilk test. Variables with non-normal distribution were expressed with median (interquartile range). Categorical data were expressed with n (%). Comparisons of continuous variables with normal distribution were tested by 1-way ANOVA with Tukey's multiple comparison, and variables with non-normal distribution were tested by Kruskal–Wallis test with Dunn's nonparametric comparison with Bonferroni adjustment. The predictive ability of $maxLCBI_{4mm}$ for no-reflow phenomenon was analyzed by receiver-operating characteristic analyses with calculations of sensitivity and specificity. The best cut-off value of $maxLCBI_{4mm}$ was determined by selecting the value which maximized the sum of sensitivity and specificity. Spearman correlation coefficient test was used to examine relationship between $maxLCBI_{4mm}$ and no-reflow phenomenon in patients with target lesions containing small and large calcification, respectively. Uni- and multivariable logistic analyses were performed to identify predictors for no-reflow phenomenon after PCI. All reported P values are 2-sided. P values < 0.05 was considered statistically significant. All statistical analyses will be performed using SPSS software version 27 (IBM®, Chicago, IL, USA).

Results

The current analysis included 272 and 189 stable CAD patients with target lesions containing small and large calcification, respectively (Supplementary Table). The averaged $maxLCBI_{4mm}$ was 435 (294, 613) (p = 0.95). Of note, over 50% of subjects with large calcification had $maxLCBI_{4mm} \geq 400$, which was similar to that at target lesions with small calcification (55.6 vs. 56.2%, p = 0.82). No-reflow phenomenon after PCI was observed in 8.0% of study subjects (small calcification: 9.9%, large

Table 1 Clinical characteristics of patients with and without no-reflow phenomenon

	No-reflow phenomenon (+) (n = 39)	No-reflow phenomenon (−) (n = 422)	p value
Age (years)	67.3 ± 11.2	69.6 ± 10.8	0.23
Female, n (%)	4 (10.3)	79 (18.7)	0.27
Body mass index (kg/m^2)	23.7 ± 3.3	24.2 ± 3.3	0.23
Hypertension, n (%)	20 (51.3)	332 (78.7)	< 0.001
Dyslipidemia, n (%)	35 (89.7)	363 (86.0)	0.63
Type 2 diabetes mellitus, n (%)	13 (33.3)	199 (47.2)	0.13
Current smoking, n (%)	9 (23.1)	79 (18.7)	0.52
Chronic kidney disease, n (%)	19 (48.7)	202 (47.9)	0.95
Hemodialysis, n (%)	2 (5.1)	26 (6.2)	0.91
A history of myocardial infarction, n (%)	17 (43.6)	108 (25.6)	0.02
A history of CABG, n (%)	2 (5.1)	21 (5.0)	1.00
Diagnosis of Stable CAD			
Angina pectoris, n (%)	12 (30.7)	122 (28.9)	0.85
Silent myocardial ischemia, n (%)	27 (69.3)	300 (71.1)	
Medication use			
Statin, n (%)	34 (87.2)	380 (90.1)	0.58
High-intensity statin, n (%)	14 (35.9)	107 (25.4)	0.18
Beta-blocker, n (%)	22 (56.4)	269 (63.7)	0.39
ACEI/ARB, n (%)	21 (53.9)	235 (55.8)	0.87
Aspirin, n (%)	35 (89.7)	400 (95.0)	0.32
P2Y12, n (%)	38 (97.4)	396 (93.8)	0.72
NIRS/IVUS-derived calcific and lipidic plaque features			
Maximum calcification arc			
0°, n (%)	9 (23.0)	68 (16.1)	0.68
0–89°, n (%)	9 (23.0)	80 (18.9)	
90–179°, n (%)	7 (18.0)	99 (23.5)	
180–269°, n (%)	7 (18.0)	99 (23.5)	
270–360°, n (%)	7 (18.0)	76 (18.0)	
Percentage of frames containing any calcification (%)	64.3 ± 41.9	67.0 ± 37.6	0.84
$MaxLCBI_{4mm}$	649 ± 252	442 ± 220	< 0.001
PCI procedures			
Filter-wire use, n (%)	9 (23.0)	7 (1.7)	< 0.001
Rotablator, n (%)	1 (2.5)	10 (2.4)	0.98
Stent diameter (mm)	3.3 ± 0.5	3.3 ± 0.6	0.49
Stent length (mm)	37.4 ± 15.2	31.0 ± 14.9	0.006

ACEI angiotensin converting enzyme inhibitor, *ARB* angiotensin II receptor blocker, *CABG* coronary artery bypass grafting, *CAD* coronary artery disease, *IVUS* intravascular ultrasound, $MaxLCBI_{4mm}$ maximum-4 mm lipid-core burden index, *NIRS* near-infrared spectroscopy imaging, *PCI* percutaneous coronary intervention

calcification: 6.9%, p = 0.30). Table 1 presented comparison of clinical characteristics in those with and without no-reflow phenomenon after PCI. Those with no-reflow phenomenon after PCI were more likely to have a history of myocardial infarction (p = 0.02), accompanied by a lower frequency of hypertension (p < 0.001) (Table 1). On NIRS/IVUS imaging analysis, while maximum calcification arc did not differ between two groups (p = 0.68),

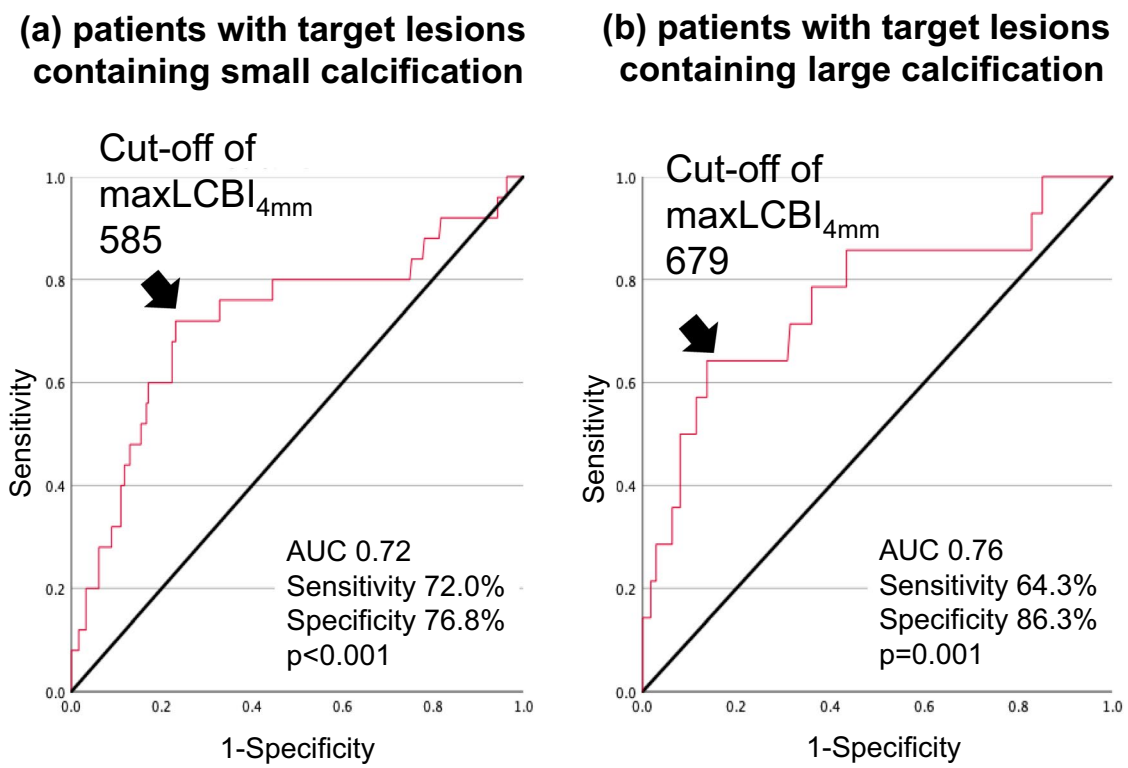

Fig. 2 ROC analysis of MaxLCBI$_{4mm}$ for predicting no-reflow phenomenon after PCI. The best cut-off value of maxLCBI$_{4mm}$ to predict no-reflow phenomenon after PCI was analyzed. **a** Patients with Target Lesions Containing Small Calcification. **b** Patients with Target Lesions Containing Large Calcification. *AUC* area under the curve, *MaxLCBI$_{4mm}$* maximum 4-mm lipid-core burden index, *PCI* percutaneous coronary intervention, *ROC* receiver-operating characteristics

a larger maxLCBI4mm was observed in patients who experienced no-reflow phenomenon after PCI (Table 1). In addition, the length of their implanted stents was longer with more frequent use of filter-wire (Table 1). Receiver-operating characteristics curve analyses were conducted to identify cut-off values of maxLCBI$_{4mm}$ at target lesions which predict no-reflow phenomenon after PCI (Fig. 2). In those with target lesions containing small calcification, its value was 585 (area under the curve: 0.72, sensitivity = 72.0%, specificity = 76.8%, $p < 0.001$). With regard to target lesions containing large calcification, 679 was a best cut-off value (area under the curve: 0.76, sensitivity = 64.3%, specificity = 86.3%, $p = 0.001$) (Fig. 2).

Clinical characteristics in patients with target lesions containing small calcification

Table 2 summarizes clinical characteristics of patients with target lesions containing small calcification stratified according to a cut-off value of maxLCBI$_{4mm}$ (585). There were no significant differences in coronary risk factors between two groups (Table 2). The frequency of guideline-recommended medications including statin was similar across the groups (Table 1).

Features of target lesions containing small calcification, and no-reflow phenomenon after PCI

Angiographic and NIRS/IVUS-derived features of target lesions containing small calcification are shown in Table 3. Over half of target lesions were located at left anterior descending artery ($p = 0.87$). Target lesions with small calcification exhibiting maxLCBI$_{4mm} \geq 585$ were more likely to have a longer lesion length ($p = 0.02$), whereas maximum calcification arc did not differ in 2 groups ($p = 0.77$). With regard to PCI procedures, they received a longer stent length ($p = 0.009$) with a greater frequency of filter-wire use ($p = 0.04$). Following the completion of PCI, minimum lesion diameter ($p = 0.54$), percent diameter stenosis ($p = 0.43$) and IVUS-derived measures of stent expansion

Table 2 Clinical characteristics of patients with target lesions containing small calcification stratified according to $MaxLCBI_{4mm}$ < and ≥ 585

	MaxLCBI < 585 (n = 196)	MaxLCBI ≥ 585 (n = 76)	p value
Age (years)	68 ± 10.8	68.5 ± 12.3	0.77
Female, n (%)	30 (15.3)	16 (21.1)	0.28
Body mass index (kg/m^2)	24.3 ± 2.9	23.9 ± 3.4	0.14
Hypertension, n (%)	146 (74.5)	54 (71.1)	0.65
Dyslipidemia, n (%)	167 (85.2)	68 (89.5)	0.43
Type 2 Diabetes Mellitus, n (%)	88 (44.9)	37 (48.7)	0.59
Current Smoking, n (%)	39 (19.9)	18 (23.7)	0.51
Chronic kidney disease, n (%)	80 (40.8)	38 (50.0)	0.18
Hemodialysis, n (%)	4 (2.0)	3 (4.0)	0.40
A history of myocardial infarction, n (%)	47 (24.0)	23 (30.3)	0.28
A history of CABG, n (%)	10 (5.1)	1 (1.3)	0.30
Diagnosis of Stable CAD			
Angina pectoris, n (%)	56 (28.6)	23 (30.3)	0.78
Silent myocardial ischemia, n (%)	140 (71.4)	53 (69.7)	
Medication Use			
Statin, n (%)	176 (89.8)	70 (92.1)	0.65
High-intensity statin, n (%)	43 (21.9)	21 (27.6)	0.34
Beta-blocker, n (%)	131 (66.8)	46 (60.5)	0.33
ACEI/ARB, n (%)	106 (54.1)	47 (61.8)	0.28
Aspirin, n (%)	186 (94.9)	72 (94.7)	0.80
P2Y12 inhibitor, n (%)	186 (94.9)	72 (94.7)	0.99

ACEI angiotensin converting enzyme inhibitor, *ARB* angiotensin II receptor blocker, *CABG* coronary artery bypass grafting, *CAD* coronary artery disease, *$MaxLCBI_{4mm}$* maximum-4 mm lipid-core burden index

(minimum stent area: p = 0.41, stent expansion rate: p = 0.40) were similar between two groups (Table 3). However, subjects with $maxLCBI_{4mm} \geq 585$ more likely exhibited a greater CTFC after PCI (p < 0.001, Table 3). Furthermore, as shown in Fig. 3, a risk of no-reflow phenomenon after PCI increased in associated with $maxLCBI_{4mm}$ (23.7% vs. 3.6%, p < 0.001, Fig. 3-a). Figure 4 illustrates the relationship of $maxLCBI_{4mm}$ with corrected TIMI frame count in patients who did not use filter-wire (n = 260). $MaxLCBI_{4mm}$ at target lesions containing small calcification were associated with CTFC (ρ = 0.32, p < 0.001, Fig. 4a).

Clinical characteristics in patients with target lesions containing large calcification

Table 4 describes clinical characteristics of patients with target lesions containing large calcification stratified according to $maxLCBI_{4mm}$ (679). Similar to those with small calcifcation, the prevalence of concomitant risk factors, angina pectoris and silent myocardial ischemia, and guideline-recommended medication use was similar in 2 groups (Table 4).

Features of target lesions containing large calcification, and no-reflow phenomenon after PCI

In patients with target lesions containing large calcification, the location of target lesions, quantitative coronary angiographic measures and the proportion of maximum calcification arc did not differ in two groups (Table 5). Filter-wire was more frequently used in those with $maxLCBI_{4mm} \geq 679$ (p = 0.01). On angiographic analysis after PCI, those with $maxLCBI_{4mm} \geq 679$ more likely exhibited larger minimum lumen diameter (p = 0.02) and corrected TIMI frame count (p < 0.001). Furthermore, large calcification with $maxLCBI_{4mm} \geq 679$ increased a risk of no-reflow phenomenon (27.3% vs. 3.2%, p < 0.001, Fig. 3b). A significant relationship between $maxLCBI_{4mm}$ at target lesions containing large calcification and CTFC existed (ρ = 0.22, p = 0.002) in subjects who did not use filter-wire (n = 185) (Fig. 4b).

Table 3 Angiographic and NIRS/IVUS characteristics, and PCI procedures in patients with target lesions containing small calcification stratified according to $MaxLCBI_{4mm}$ < and ≥ 585

	MaxLCBI < 585 (n = 196)	MaxLCBI ≥ 585 (n = 76)	p value
Location of culprit lesions			
LAD, n (%)	114 (58.2)	45 (59.2)	0.87
LCX, n (%)	28 (14.3)	13 (17.1)	
RCA, n (%)	52 (26.5)	52 (23.7)	
LMT, n (%)	1 (0.5)	0 (0.0)	
SVG, n (%)	1 (0.5)	0 (0.0)	
Pre PCI measures			
Quantitative coronary angiography analysis			
Reference diameter (mm)	3.0 ± 0.6	2.9 ± 0.7	0.31
MLD (mm)	0.8 ± 0.5	0.7 ± 0.4	0.47
%DS (%)	71.0 ± 16.6	72.4 ± 16.5	0.48
Lesion length (mm)	18.4 ± 10.7	23.8 ± 14.8	0.02
NIRS/IVUS-derived calcific and lipidic plaque features			
Maximum calcification arc			
0°, n (%)	54 (27.6)	23 (30.3)	0.77
0–89°, n (%)	63 (32.1)	26 (34.2)	
90–179°, n (%)	79 (40.3)	27 (35.5)	
Percentage of frames containing any calcification (%)	51.5 ± 37.9	47.6 ± 36.9	0.55
$MaxLCBI_{4mm}$	347 ± 143	766 ± 111	< 0.001
PCI Procedures			
Filter-wire use, n (%)	5 (2.6)	7 (9.2)	0.04
Rotablator, n (%)	4 (2.1)	0 (0)	0.58
Stent diameter (mm)	3.2 ± 0.5	3.2 ± 0.6	0.78
Stent length (mm)	29.5 ± 14.4	34.8 ± 16.7	0.009
Post-dilatation after stent implantation (%)	160 (81.6)	64 (84.2)	0.71
Diameter of balloon for post-dilatation (mm)	3.4 ± 0.4	3.3 ± 0.4	0.69
Post PCI measures			
Quantitative coronary angiography analysis			
MLD after PCI (mm)	2.8 ± 0.5	2.8 ± 0.6	0.54
%DS after PCI (%)	10.0 ± 7.8	8.9 ± 7.3	0.43
Corrected TIMI frame count	9.8 ± 5.3	17.0 ± 11.4	< 0.001
The degree of stent expansion on IVUS imaging			
MSA after PCI (mm^2)	6.5 ± 2.5	6.1 ± 2.0	0.41
Stent expansion (%)	83.6 ± 18.6	81.8 ± 15.4	0.40

IVUS intravascular ultrasound, *LAD* left anterior descending artery, *LCX* left circumflex artery, *MaxLCBI$_{4mm}$* maximum-4 mm lipid-core burden index, *MLD* minimum lesion diameter, *MSA* minimum stent area, *NIRS* near-infrared spectroscopy imaging, *PCI* percutaneous coronary intervention, *%DS* percent diameter stenosis, *RCA* right coronary artery, *SVG* saphenous vein graft

Predictors of no-reflow phenomenon after PCI

Uni- and multivariable logistic analyses were conducted to elucidate predictors of no-reflow phenomenon after PCI (Table 6). In patients with target lesions containing small calcification, univariate analysis showed age [odds ratio (OR) = 0.96, 95% confidence interval (CI) = 0.92–0.99, p = 0.03], a history of hypertension (OR = 0.34, 95%CI = 0.15–0.80, p = 0.01) and $maxLCBI_{4mm}$ (OR = 1.41, 95%CI = 1.25–1.68, p < 0.001) as significant predictors

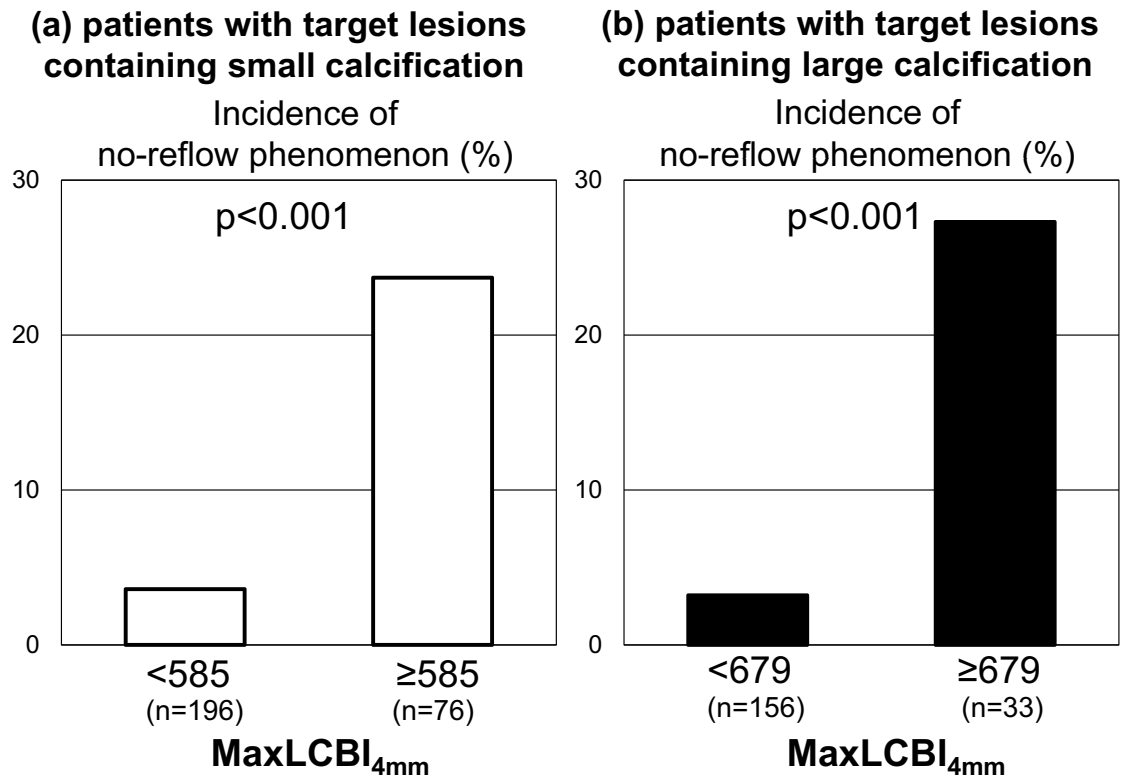

Fig. 3 Incidence of no-reflow phenomenon. Incidence of no-reflow phenomenon after PCI was compared in subjects stratified according to $maxLCBI_{4mm}$ at target lesions. **a** Patients with Target Lesions Containing Small Calcification. **b** Patients with Target Lesions Containing Large Calcification. *MaxLCBI*$_{4mm}$ maximum 4-mm lipid-core burden index

(Table 6-a). Even after adjusting age, female gender, a history of hypertension, %DS after PCI and MSA, $maxLCBI_{4mm}$ remained an independent predictor of no-reflow phenomenon (OR = 1.35, 95%CI 1.14–1.63, p = 0.007, Table 6a). In patients with target lesions containing large calcification, following adjustment of clinical characteristics (age, female gender, a history of hypertension, %DS after PCI and MSA), $maxLCBI_{4mm}$ still continued to associate with no-reflow phenomenon (OR = 1.60, 95%CI = 1.32–1.94, p < 0.001, Table 6b). Figure 5 illustrates two representative cases.

Discussion

Calcified lesion has been characterized as quiescent atheroma with a lower risk of no-reflow phenomenon after PCI. In the current study, however, this PCI-related complication occurred even at target lesions containing large calcification in stable CAD patients. A risk of no-reflow phenomenon after PCI at those with large calcification was driven by the degree of lipidic materials. $MaxLCBI_{4mm}$ on NIRS imaging was an independent predictor of no-reflow phenomenon even after adjustment of clinical, angiographic and IVUS features. Our findings suggest that lipidic materials could exist within calcified lesions and associate with an increased risk of no-reflow phenomenon after PCI with DES implantation.

Pathohistological studies have shown that calcification presents around inflamed lipid-rich necrotic cores [4–9], whereas in vivo studies exploring the colocalization of these plaque features were limited. The current study employed NIRS imaging which enables to evaluate lipidic materials under overlying calcification due to the ability of near-infrared light to penetrate calcification. We observed that 55.6% of calcified target lesions exhibited $maxLCBI_{4mm} > 400$, a signature of lipid-rich lesion, in stable CAD patients, and this frequency was similar to that at non-calcified target lesions (= 56.2%). The interactions between calcific and

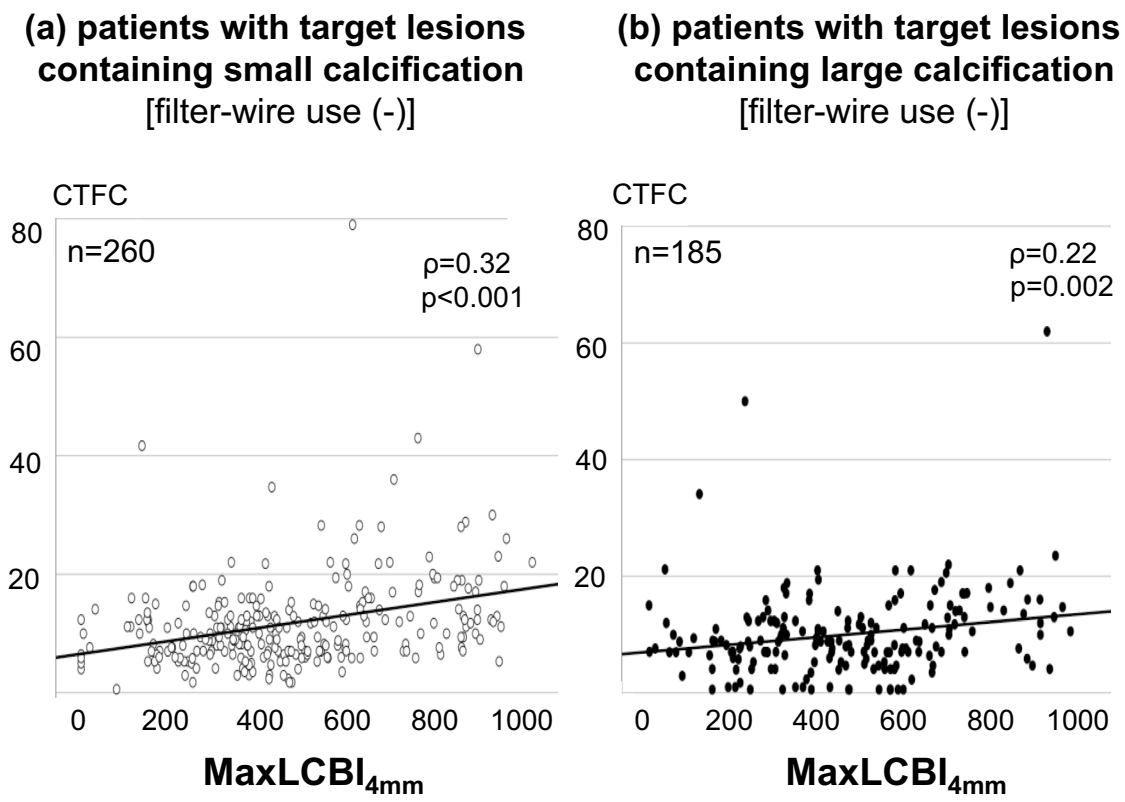

Fig. 4 Relationship of $MaxLCBI_{4mm}$ with CTFC in patients without filter-wire use. Spearman correlation analysis was performed to investigate the relationship between $maxLCBI_{4mm}$ and CTFC in patients receiving PCI without filter-wire use. **a** Patients with Target Lesions Containing Small Calcification (n = 260). **b** Patients with Target Lesions Containing Large Calcification (n = 185). *CTFC* corrected thrombolysis in myocardium infarction frame count, *MaxLCBI*$_{4mm}$ maximum 4-mm lipid-core burden index

lipidic plaque components have been recently reported by one recent study conducting frame-based analysis. This study reported the presence of both calcium and lipids at 9.3% of analyzed frames at non-culprit segments in 139 patients with CAD selected from the IBIS-3 study [14]. The frequency of colocalized calcium and lipid varies in this and our studies partly due to different analytic method and evaluated lesions. However, these findings highlight that calcified lesion is not necessarily quiescent atheroma, but it could exhibit active form harboring lipidic material. Whether a risk of future coronary events differs in calcified lesions with and without lipidic plaque components requires further investigation.

The current study observed an increased risk of no-reflow phenomenon at lesions containing large calcification in association with the degree of lipidic materials. Furthermore, the relationship between deteriorated coronary flow and $maxLCBI_{4mm}$ at lesions containing large calcification was identified. Mechanistically, a dynamic fracture of overlying calcification after DES implantation might occur, which allows lipidic materials within the lesions to embolize and then cause deterioration of coronary flow. It could be speculated thickness of calcification as a potential contributor to this PCI-related modification of calcified lesions. Due to a limited resolution of IVUS, the current study was not able to investigate how calcification overlying lipidic plaque components behaved PCI. Further characterization of calcification is warranted by using other imaging technique.

Intravascular imaging modalities have been shown as a tool to estimate a risk of no-reflow phenomenon after PCI [2, 19, 20]. A greater frequency of no-reflow phenomenon was observed at lesions with IVUS-derived ultrasound attenuation [16], necrotic core visualized by VH-IVUS [20] or lipid plaque on OCT imaging [2]. In the current study, $maxLCBI_{4mm}$ at lesions with both small and large calcification predicted this PCI-related complication. $MaxLCBI_{4mm}$

Table 4 Clinical characteristics of patients with target lesions containing large calcification stratified according to $MaxLCBI_{4mm}$ < and ≥ 679

	maxLCBI < 679 (n = 156)	maxLCBI ≥ 679 (n = 33)	p value
Age (years)	70.6 ± 10.3	72.9 ± 9.3	0.26
Female, n (%)	33 (21.2)	4 (12.1)	0.33
Body mass index (kg/m^2)	23.9 ± 3.8	24.4 ± 3.2	0.38
Hypertension, n (%)	126 (80.8)	26 (78.8)	0.81
Dyslipidemia, n (%)	135 (86.5)	28 (84.9)	0.78
Type 2 Diabetes Mellitus, n (%)	74 (47.4)	13 (39.4)	0.45
Current Smoking, n (%)	27 (17.3)	4 (12.1)	0.61
Chronic kidney disease, n (%)	87 (55.8)	16 (48.5)	0.45
Hemodialysis, n (%)	18 (11.5)	3 (9.1)	0.90
A history of myocardial infarction, n (%)	43 (27.6)	12 (36.4)	0.40
A history of CABG, n (%)	10 (6.4)	2 (6.1)	0.98
Diagnosis of Stable CAD			
Angina pectoris, n (%)	45 (28.8)	10 (30.4)	0.77
Silent myocardial ischemia, n (%)	111 (71.2)	23 (69.6)	
Medication Use			
Statin, n (%)	137 (87.8)	31 (93.9)	0.54
High-intensity statin, n (%)	49 (31.4)	8 (24.2)	0.53
Beta-blocker, n (%)	94 (60.3)	20 (60.6)	0.98
ACEI/ARB, n (%)	86 (55.5)	17 (51.5)	0.70
Aspirin, n (%)	147 (94.8)	30 (90.9)	0.41
P2Y12, n (%)	144 (92.3)	32 (97.0)	0.47

ACEI angiotensin converting enzyme inhibitor, *ARB* angiotensin II receptor blocker, *CABG* coronary artery bypass grafting, *CAD* coronary artery disease, *$MaxLCBI_{4mm}$* maximum-4 mm lipid-core burden index

has been histologically validated to reflect the presence of lipid-rich plaque [10–14], and this NIRS-derived measure corresponds to the aforementioned plaque features visualized by IVUS, VH-IVUS or OCT [21, 22]. These collective findings support the potential of NIRS imaging to identify high-risk coronary lesions causing no-reflow phenomenon after PCI.

There are several published studies which reported cut-off values of NIRS-derived measure to predict no-reflow phenomenon. Goldstein, et al. analyzed the relationship of $maxLCBI_{4mm}$ with periprocedural myocardial infarction in 62 CAD patients receiving PCI [23]. In this analysis, $maxLCBI_{4mm} \geq 500$ was a predictor of periprocedural myocardial infarction. The another study investigated the predictive ability of a novel index, total LCBI/$maxLCBI_{4mm}$ ratio for filter-no-reflow phenomenon in 32 ACS patients [24]. Total LCBI/$maxLCBI_{4mm}$ ratio > 0.42 was an independent predictor of filter-no-reflow phenomenon. While these studies revealed clinical applicability of $maxLCBI_{4mm}$ to estimate a risk of PCI-related complication risk, whether calcification affects the relationship of this NIRS-derived measure with no-reflow phenomenon has not been investigated. The current findings provide additional evidence which indicates $maxLCBI_{4mm}$ at calcified lesions as a tool to stratify a risk of no-reflow phenomenon after PCI.

High $maxLCBI_{4mm}$ at calcified lesions underscores adjunctive management to mitigate a risk of no-reflow phenomenon in stable CAD patients receiving PCI. We reported a case using a filter-wire at severely calcified lesion with substantially elevated $maxLCBI_{4mm}$, which was effective to prevent coronary flow deterioration after DES [25]. More awareness is required for interventionalists to consider embolic protection device for treating calcified target lesions containing lipid-rich materials in stable CAD patients. However, this approach is not available when rotational or orbital atherectomy is used to modulate severe calcification. It may be better to consider debulking procedure which focuses on a limited segment with appropriate size of device and rotational/orbital speed. Given a greater frequency of

Table 5 Angiographic and NIRS/IVUS characteristics, and PCI procedures in patients with target lesions containing large calcification stratified according to $MaxLCBI_{4mm}$ < and ≥ 679

	maxLCBI < 679 (n = 156)	maxLCBI ≥ 679 (n = 33)	p value
Location of culprit lesions			
LAD, n (%)	100 (64.1)	17 (51.5)	0.62
LCX, n (%)	18 (11.5)	6 (18.2)	
RCA, n (%)	35 (22.4)	1 (3.0)	
LMT, n (%)	2 (1.3)	0 (0.0)	
SVG, n (%)	1 (0.7)	9 (27.3)	
Pre PCI measures			
Quantitative coronary angiography analysis			
Reference diameter (mm)	2.9 ± 0.7	3.2 ± 0.8	0.10
MLD (mm)	0.8 ± 0.4	0.71 ± 0.4	0.18
%DS (%)	70.9 ± 14.2	76.0 ± 13.0	0.10
Lesion length (mm)	19.3 ± 12.7	23.8 ± 15.6	0.17
NIRS/IVUS-derived calcific and lipidic plaque features			
Maximum calcification arc			
180–269°, n (%)	89 (57.1)	17 (51.5)	0.57
270–360°, n (%)	67 (42.9)	16 (48.5)	
Percentage of frames containing any calcification (%)	96.0 ± 11.7	97.6 ± 8.8	0.50
$MaxLCBI_{4mm}$	379 ± 172	800 ± 93	< 0.001
PCI procedures			
Filter-wire use, n (%)	1 (0.6)	3 (9.1)	0.01
Rotablator, n (%)	5 (3.2)	2 (6.1)	0.35
Stent diameter (mm)	3.3 ± 0.6	3.5 ± 0.6	0.56
Stent length (mm)	31.6 ± 14.1	36.0 ± 16.6	0.24
Post-dilatation after stent implantation (%)	148 (94.8)	31 (93.9)	0.90
Diameter of balloon for post-dilatation (mm)	3.4 ± 0.5	3.6 ± 0.6	0.69
Post PCI measures			
Quantitative coronary angiography analysis			
MLD after PCI (mm)	2.7 ± 0.6	3.0 ± 0.5	0.02
%DS after PCI (%)	11.6 ± 11.2	9.8 ± 7.1	0.68
Corrected TIMI frame count	9.0 ± 6.3	14.9 ± 9.6	< 0.001
The degree of stent expansion on IVUS imaging			
MSA after PCI (mm^2)	6.6 ± 2.2	6.2 ± 2.3	0.37
Stent expansion (%)	79.2 ± 20.5	78.1 ± 14.0	0.63

IVUS intravascular ultrasound, *LAD* left anterior descending artery, *LCX* left circumflex artery, *MaxLCBI$_{4mm}$* maximum-4 mm lipid-core burden index, *MLD* minimum lesion diameter, *MSA* minimum stent area, *NIRS* near-infrared spectroscopy imaging, *PCI* percutaneous coronary intervention, *%DS* percent diameter stenosis, *RCA* right coronary artery, *SVG* saphenous vein graft

$maxLCBI_{4mm} > 400$ even at target lesions containing large calcification, more intensified lipid-lowering therapies are required prior to PCI.

IVUS enables to detect calcification. However, this modality is limited to quantify calcification volume due to acoustic shadowing. Other invasive and non-invasive imaging (optical coherence tomography, computed tomography, etc.) are capable of visualizing calcification but not measuring its volume. Novel imaging approach quantifying calcification volume is required to further elucidate whether calcification volume itself affects the relationship between $maxLCBI_{4mm}$ and no-reflow phenomenon.

Table 6 Predictors of no-reflow phenomenon

Variables	OR	95%CI	p value	Variables	OR	95%CI	p value
Patients with non-calcified target lesions							
Age	0.96	0.92–0.99	0.03	Age	0.9	0.91–0.99	0.04
Female	0.66	0.19–2.31	0.51	Female	1.213	0.24–6.12	0.81
Body mass index	1.01	0.87–1.15	0.91	–	–	–	–
Hypertension	0.34	0.15–0.80	0.01	Hypertension	0.35	0.12–1.03	0.06
Dyslipidemia	1.90	0.43–8.45	0.39	–	–	–	–
Type 2 Diabetes Mellitus	0.52	0.21–1.26	0.15	–	–	–	–
Chronic kidney disease	1.02	0.44–2.33	0.96	–	–	–	–
Statin	0.75	0.21–2.72	0.66	–	–	–	–
%DS	0.99	0.97–1.02	0.87	–	–	–	–
MLD	1.35	0.49–3.70	0.55	–	–	–	–
Lesion length	1.01	0.97–1.04	0.62	–	–	–	–
Calcium score	0.73	0.44–1.21	0.23	–	–	–	–
$MaxLCBI_{4mm}$ per 100	1.41	1.25–1.68	< 0.001	$MaxLCBI_{4mm}$ per 100	1.35	1.14–1.63	0.007
%DS after PCI	1.05	0.99–1.11	0.06	%DS after PCI	1.05	0.99–1.12	0.07
MLD after PCI	0.75	0.30–1.87	0.54	–	–	–	–
MSA	1.08	0.92–1.26	0.30	MSA	1.18	0.99–1.40	0.06
% stent expansion	1.01	0.98–1.03	0.35	–	–	–	–
Patients with calcified target lesions							
Age	1.02	0.97–1.08	0.36	Age	1.05	0.97–1.14	0.18
Female	0.29	0.03–2.34	0.25	Female	0.31	0.01–1.34	0.55
Body mass index	0.86	0.72–1.04	0.13	–	–	–	–
Hypertension	0.20	0.06–0.63	0.006	Hypertension	0.08	0.01–0.43	0.003
Dyslipidemia	0.95	0.20–4.52	0.95	–	–	–	–
Type 2 Diabetes Mellitus	0.63	0.20–1.95	0.42	–	–	–	–
Chronic kidney disease	1.12	0.37–3.37	0.83	–	–	–	–
Statin	0.73	0.15–3.51	0.69	–	–	–	–
%DS	1.02	0.98–1.06	0.27	–	–	–	–
MLD	0.71	0.14–3.66	0.69	–	–	–	–
Lesion length	0.99	0.95–1.04	0.92	–	–	–	–
Calcium score	1.30	0.43–3.87	0.63	–	–	–	–
$MaxLCBI_{4mm}$ per 100	1.65	1.44–2.01	< 0.001	$MaxLCBI_{4mm}$ per 100	1.60	1.32–1.94	< 0.001
%DS after PCI	0.98	0.92–1.04	0.59	–	–	–	–
MLD after PCI	1.31	0.49–3.48	0.58	–	–	–	–
MSA	0.87	0.65–1.16	0.35	MSA	0.89	0.63–1.26	0.52
% stent expansion	0.99	0.967–1.02	0.86	–	–	–	–

$MaxLCBI_{4mm}$ maximum-4 mm lipid-core burden index, *MLD* minimum lesion diameter, *MSA* minimum stent area, *%DS* percent diameter stenosis, *RCA* right coronary artery

Study limitations

Several caveats should be considered to interpret the current findings. Firstly, this is a retrospective cross-sectional observational study from a registry database which enrolled stable CAD patients using NIRS/IVUS imaging for PCI, therefore selection bias could not be excluded. Secondly, procedural strategy including filter-wire was decided according to each PCI operator. This may be bias affecting PCI outcomes. Thirdly, the current study included stable CAD patients only. The cut-off values of $maxLCBI_{4mm}$ at target lesions for predicting no-reflow phenomenon may be different in ACS patients. Fourth, IVUS does not have capability to evaluate thickness and volume of calcification. It remains unknown whether these features of calcification could affect the current findings. Fifth, the current study evaluated CTFC immediately after DES

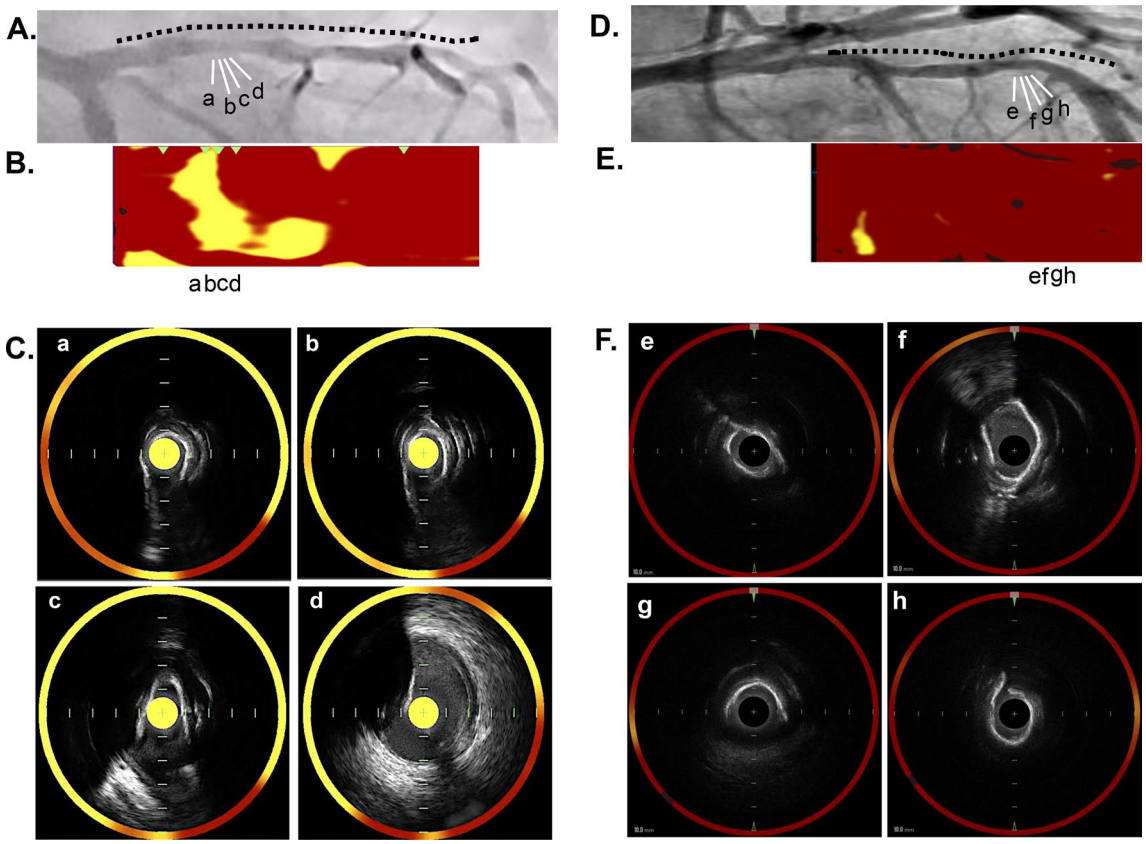

Fig. 5 Representative cases. **A** A 67-year old gentleman presented stable angina pectoris. The proximal segment of his LAD was treated by PCI. Black dotted line was the imaged segments with NIRS/IVUS. a, b, c and d correspond to images in **B** and **C**. **B** NIRS imaging prior to PCI visualized the presence of lipidic plaque materials at the calcified target lesion, and maxLCBI$_{4mm}$ was 817. **C** Cross-sectional images (**D**) showed the extensive yellow signals at the corresponding calcified lesion. The maximum calcification arc was 297°. After stent implantation, no-reflow phenomenon occurred. **D** A 58-yearl old gentleman received an elective PCI to treat moderate stenosis at the middle segment of his LAD. Black dotted line was the imaged segments with NIRS/IVUS. e, f, g and h correspond to images in **E** and **F**. **E** MaxLCBI$_{4mm}$ at this lesion was 83. **F** On NIRS/IVUS cross-sectional imaging, calcification arc was 360° (**H**), accompanied by very small amount of yellow signals. No-reflow phenomenon did not occur after PCI. *IVUS* intravascular ultrasound, *LAD* left anterior descending artery, *MaxLCBI$_{4mm}$* maximum 4-mm lipid-core burden index, *NIRS* near-infrared spectroscopy, *PCI* percutaneous coronary intervention

implantation but not pre-dilatation or debulking procedure. This is because coronary flow could be deteriorated due to severe dissection and/or thrombus caused by plain old balloon angioplasty and/or rotational/orbital atherectomy. Therefore, it remains unknown the frequency of no-reflow phenomenon after procedure prior to DES implantation. Sixth, the size of NIRS imaging catheter's shaft is a larger compared to other IVUS catheter (Altaview™, Terumo, Japan) and OCT. In addition, since NIRS/IVUS catheter has a fiber cable which emits near-infrared light, this makes its catheter less flexible. These features of NIRS/IVUS imaging catheter makes difficult to cross lesions containing heavy calcification. In the current study, NIRS/IVUS was not used at lesions exhibiting very severe calcification. Therefore, it remains unknown about the frequency and characteristics of lipidic plaque materials at lesions containing very severe calcification.

Conclusions

In the present study analyzing stable CAD patients, maxLCBI$_{4mm}$ at lesions containing small calcification predicted the occurrence of no-reflow phenomenon after PCI. Of note, even at target lesions harboring large calcification, 55.6% of those exhibited maxLCBI$_{4mm}$ > 400. Moreover, despite features of calcification, maxLCBI$_{4mm}$ at target lesions with large calcification was associated with a higher CTFC and a greater frequency of no-reflow phenomenon after PCI. Our findings suggest that calcified plaque concomitantly harbors lipidic plaque materials in vivo. Calcified plaque containing lipidic materials is not necessarily stable lesion, but could be active and high-risk one causing no-reflow phenomenon.

Supplementary Information The online version contains supplementary material available at https://doi.org/10.1007/s10554-023-02905-y.

Acknowledgements We would like to acknowledge cardiology medical fellows and co-medical staffs (Sayaka Watanabe, Shintaro Kobayashi and Tomoyuki Kondo) for their support to conduct NIRS/IVUS imaging during PCI. We thank Miss Yuko Yoshioka and Miss Emi Kanai for their excellent assistance.

Authors contributions All authors contributed to the study conception and design. Material preparation, data collection and analysis were performed by HH and YK. The first draft of the manuscript was written by HH and YK and all authors commented on previous versions of the manuscript. All authors read and approved the final manuscript.

Funding This study was supported by 2021 research grant of Nakatani Foundation for advancement of measuring technologies in biomedical engineering, and JSPS KAKENHI Grant number JP20K08415.

Availability of data and materials The data sharing underlying this article requires the approval of principal investigator and the research ethics committee at National Cerebral & Cardiovascular Center.

Declarations

Competing interests Yu Kataoka has received research support from Nipro and Abbott, and and honoraria from Nipro, Abbott, Kowa, Amgen, Sanofi, Astellas, Takeda and Daiichi-Sankyo. Other authors have nothing to disclose.

Conflict of interest Yu Kataoka has received research support from Nipro and Abbott, and and honoraria from Nipro, Abbott, Kowa, Amgen, Sanofi, Astellas, Takeda and Daiichi-Sankyo. Other authors have nothing to disclose.

Ethical approval This study was approved by the institutional review board of the National Cerebral and Cardiovascular Center (M30-084-4), the Miyazaki Medical Association Hospital (2020-43) and Sakakibara Heart Institute. Written informed consent was not obtained in each subject due to the observational analysis of hospitalized patients.

References

1. Tanaka A, Kawarabayashi T, Nishibori Y, Sano T, Nishida Y, Fukuda D et al (2002) No-reflow phenomenon and lesion morphology in patients with acute myocardial infarction. Circulation 105:2148–2152
2. Soeda T, Higuma T, Abe N, Yamada M, Yokoyama H, Shibutani S et al (2017) Morphological predictors for no reflow phenomenon after primary percutaneous coronary intervention in patients with ST-segment elevation myocardial infarction caused by plaque rupture. Eur Heart J Cardiovasc Imaging 18:103–110
3. Patel VG, Brayton KM, Mintz GS, Maehara A, Banerjee S, Brilakis ES (2013) Intracoronary and noninvasive imaging for prediction of distal embolization and periprocedural myocardial infarction during native coronary artery percutaneous intervention. Circ Cardiovasc Imaging 6:1102–1114
4. Otsuka F, Sakakura K, Yahagi K, Joner M, Virmani R (2014) Has our understanding of calcification in human coronary atherosclerosis progressed? Arterioscler Thromb Vasc Biol 34:724–736
5. Abedin M, Tintut Y, Demer LL (2004) Vascular calcification: mechanisms and clinical ramifications. Arterioscler Thromb Vasc Biol 24:1161–1170
6. Hirota S, Imakita M, Kohri K, Ito A, Morii E, Adachi S et al (1993) Expression of osteopontin messenger RNA by macrophages in atherosclerotic plaques. Am J Pathol 143:1003–1008
7. Boström K, Watson KE, Horn S, Wortham C, Herman IM, Demer LL (1993) Bone morphogenetic protein expression in human atherosclerotic lesions. J Clin Invest 91:1800–1809
8. Aikawa E, Nahrendorf M, Figueiredo JL, Swirski FK, Shtatland T, Kohler RH et al (2007) Osteogenesis associates with inflammation in early-stage atherosclerosis evaluated by molecular imaging in vivo. Circulation 116:2841–2850
9. Tintut Y, Patel J, Parhami F, Demer LL (2000) Tumor necrosis factor-alpha promotes in vitro calcification of vascular cells via the cAMP pathway. Circulation 102:2636–2642
10. Madder RD, Puri R, Muller JE, Harnek J, Götberg M, VanOosterhout S et al (2016) Confirmation of the intracoronary near-infrared spectroscopy threshold of lipid-rich plaques that underlie ST-segment-elevation myocardial infarction. Arterioscler Thromb Vasc Biol 36:1010–1015
11. Gardner CM, Tan H, Hull EL, Lisauskas JB, Sum ST, Meese TM et al (2008) Detection of lipid core coronary plaques in autopsy specimens with a novel catheter-based near-infrared spectroscopy system. JACC Cardiovasc Imaging 1:638–648
12. Wang J, Geng YJ, Guo B, Kilma T, Lal BN, Willerson JT et al (2002) Near-infrared spectroscopic characterization of human advanced atherosclerotic plaques. J Am Coll Cardiol 39:1305–1313
13. Waxman S, Dixon SR, L'Allier P, Moses JW, Petersen JL, Cutlip D et al (2009) In vivo validation of a catheter-based near-infrared spectroscopy system for detection of lipid core coronary plaques: initial results of the SPECTACL study. JACC Cardiovasc Imaging 2:858–868
14. Hartman EMJ, Hoogendoorn A, Akyildiz AC, Schuurman AS, van der Steen AFW, Boersma E et al (2020) Colocalization of intracoronary lipid-rich plaques and calcifications: an integrated NIRS-IVUS analysis. JACC Cardiovasc Imaging 13:1627–1628
15. Gibson CM, Cannon CP, Daley WL, Dodge JT, Alexander B, Marble SJ et al (1996) TIMI frame count: a quantitative method of assessing coronary artery flow. Circulation 93:879–888
16. Endo M, Hibi K, Shimizu T, Komura N, Kusama I, Otsuka F et al (2010) Impact of ultrasound attenuation and plaque rupture as detected by intravascular ultrasound on the incidence of no-reflow phenomenon after percutaneous coronary intervention in ST-segment elevation myocardial infarction. JACC Cardiovasc Interv 3:540–549
17. Zhang J, Gao X, Kan J, Ge Z, Han L, Lu S et al (2018) Intravascular ultrasound versus angiography-guided drug-eluting stent implantation: the ULTIMATE trial. J Am Coll Cardiol 72:3126–3137
18. Mintz GS, Nissen SE, Anderson WD, Bailey SR, Erbel R, Fitzgerald PJ et al (2001) American College of Cardiology

Clinical Expert Consensus Document on Standards for Acquisition, Measurement and Reporting of Intravascular Ultrasound Studies (IVUS). A report of the American College of Cardiology Task Force on Clinical Expert Consensus Documents. J Am Coll Cardiol 37:1478–1492
19. Tanaka A, Imanishi T, Kitabata H, Kubo T, Takarada S, Tanimoto T et al (2009) Lipid-rich plaque and myocardial perfusion after successful stenting in patients with non-ST-segment elevation acute coronary syndrome: an optical coherence tomography study. Eur Heart J 30:1348–1355
20. Hong YJ, Jeong MH, Choi YH, Ko JS, Lee MG, Kang WY et al (2011) Impact of plaque components on no-reflow phenomenon after stent deployment in patients with acute coronary syndrome: a virtual histology-intravascular ultrasound analysis. Eur Heart J 32:2059–2066
21. Pu J, Mintz GS, Biro S, Lee JB, Sum ST, Madden SP et al (2014) Insights into echo-attenuated plaques, echolucent plaques, and plaques with spotty calcification: novel findings from comparisons among intravascular ultrasound, near-infrared spectroscopy, and pathological histology in 2,294 human coronary artery segments. J Am Coll Cardiol 63:2220–2233
22. Zanchin C, Ueki Y, Losdat S, Fahrni G, Daemen J, Ondracek AS et al (2021) In vivo relationship between near-infrared spectroscopy-detected lipid-rich plaques and morphological plaque characteristics by optical coherence tomography and intravascular ultrasound: a multimodality intravascular imaging study. Eur Heart J Cardiovasc Imaging 22:824–834
23. Goldstein JA, Maini B, Dixon SR, Brilakis ES, Grines CL, Rizik DG et al (2011) Detection of lipid-core plaques by intracoronary near-infrared spectroscopy identifies high risk of periprocedural myocardial infarction. Circ Cardiovasc Interv 4:429–437
24. Sato T, Aizawa Y, Suzuki N, Taya Y, Yuasa S, Kishi S et al (2018) The utility of total lipid core burden index/maximal lipid core burden index ratio within the culprit plaque to predict filter-no reflow: insights from near-infrared spectroscopy with intravascular ultrasound. J Thromb Thrombolysis 46:203–210
25. Hosoda H, Kataoka Y, Otsuka F, Yasuda S (2019) Severely calcified lipidic atheroma on intravascular ultrasound and near-infrared spectroscopy imaging: its association with slow-flow phenomenon during percutaneous coronary intervention. Eur Heart J Case Rep 3:ytz078